



# Porous Scaffolds for Electrochemically Controlled Reversible Capture and Release of Ethylene

Lukasz Mendecki, Michael Ko, Xiaoping Zhang, Zheng Meng, and Katherine A. Mirica\*

Department of Chemistry, Dartmouth College, Hanover, New Hampshire 03755, United States

 Supporting Information

**ABSTRACT:** This Communication describes the use of porous coordination polymers (PCP) with integrated metal bis(dithiolene) units to achieve electrochemically controlled capture and release of ethylene in the solid state. Applying positive potential (+2.0 V) to these PCPs promotes ethylene capture, and subsequent dose of negative potential (−2.0 V) induces the release. These materials are resistant to poisoning by small reactive gases (CO and H<sub>2</sub>S) that may interact with embedded metallic sites.

Worldwide demand for ethylene exceeds that of any other organic chemical.<sup>1,2</sup> Extraction of ethylene from petroleum, however, is an energy-demanding process that involves steam cracking and cryogenic distillation.<sup>3</sup> Alternatives that utilize transition metal complexes can improve energy-efficiency, but suffer from poisoning—and the reduction in performance—triggered by H<sub>2</sub>, C<sub>2</sub>H<sub>2</sub>, CO, and H<sub>2</sub>S.<sup>4,5</sup> Growing environmental concerns require improved methods for separating alkenes from petrochemical feedstocks.<sup>6,7</sup>

In 2001, Wang and Stiefel<sup>8</sup> proposed a strategy for purifying alkenes from a multicomponent gas stream using an electrochemically controlled cycloaddition reaction<sup>8,9</sup> with metal bis(dithiolene) complexes.<sup>10</sup> The implementation of this strategy in purification, however, has remained elusive, and has been limited to computational studies and demonstrations in solution using molecular complexes.<sup>11–18</sup> Achieving reversible electrochemically controlled capture of ethylene at the solid–gas interface can lead to improved methods of alkene separation.<sup>19,20</sup>

This paper describes an experimental demonstration of using porous coordination polymers (PCPs) for reversible electrochemically driven capture of ethylene. The molecular design features the integration of the metal bis(dithiolene) units into d– $\pi$  conjugated, conductive, electrochemically active PCPs (Figure 1). Though this class of materials has been shown to exhibit promising electrocatalytic,<sup>21–24</sup> electronic,<sup>25–28</sup> and magnetic properties,<sup>29–31</sup> its function in reversible electrochemical molecular capture has not been shown. We used reticular synthesis through the reaction between 2,3,6,7,10,11-hexathiatriphenylene (HHTTP) linkers and divalent metal ions (M<sup>2+</sup>) supplied in the form of cobalt(II) acetate, nickel(II) acetate, or copper(II) trifluoroacetylacetonate, under basic conditions (pH 10) to generate M<sub>3</sub>HHTTP<sub>2</sub> PCPs (Figure 1A).<sup>22,29</sup> To probe the role of the chalcogen atom (S vs O), and the role of the metal in voltage-actuated capture, 2,3,6,7,10,11-

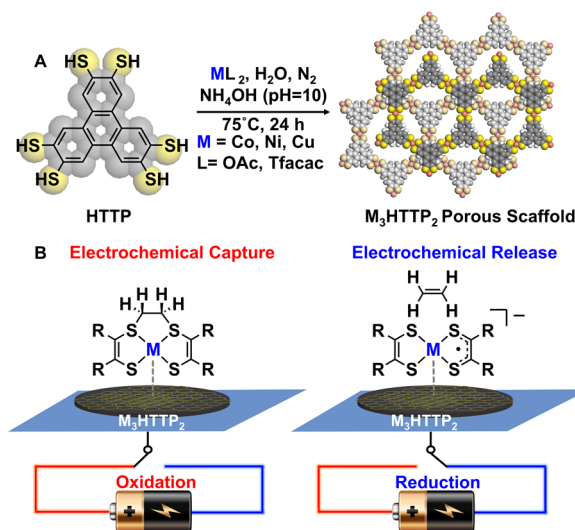


**Figure 1.** (A) Synthesis of PCPs. (B) Illustration of proposed voltage-actuated capture and release of ethylene with PCPs.

hexahydroxytriphenylene (HHTTP)-based analogs, M<sub>3</sub>HHTTP<sub>2</sub> metal–organic frameworks (MOFs), were also tested (See SI for details).<sup>32–34</sup>

Inductively coupled plasma mass spectrometry (ICP-MS) quantified the metal content in the bulk to be consistent with the molecular formula of M<sub>3</sub>HHTTP<sub>2</sub> (Tables S1–S3). X-ray photoelectron spectroscopy (XPS) demonstrated mixed valency in Co<sub>3</sub>HHTTP<sub>2</sub> (Co<sup>2+</sup>/Co<sup>3+</sup>) and in Cu<sub>3</sub>HHTTP<sub>2</sub> (Cu<sup>1+</sup>/Cu<sup>2+</sup>), with only Ni<sup>2+</sup> present in Ni<sub>3</sub>HHTTP<sub>2</sub> (Figures S8–S10). XPS also revealed the presence of NH<sub>4</sub><sup>+</sup> counterions, consistent with the anionic form of [M<sub>3</sub>HHTTP<sub>2</sub>]<sup>−</sup> subunits, and the presence of O-containing defects in the form of sulfates and sulfites (Figures S8–S10). These findings are consistent with recent reports of similar materials.<sup>21,22,35</sup> Combustion analysis quantified the amount of S, C, and N in the bulk (Tables S1–S3). S, C, M (Co, Ni, Cu), and O were also observed by energy-dispersive X-ray spectroscopy (EDS, Figure S4C).

Scanning electron microscopy (SEM) revealed nonuniform nanoscale morphologies of PCPs (Figure S4A). Powder X-ray diffraction (pXRD) showed limited crystallinity, with broad peak at 2 $\theta$  = 9.0°, consistent with the pore dimensions of 2.0 nm. This peak was absent in the pXRD analysis of the HHTTP-based molecular precursor (Figure S4B).<sup>21</sup> The Ni- and Cu-

Received: August 1, 2017

PCP analogs also showed a [001] peak at  $2\theta = 21.5^\circ$ , consistent with layered structure with an interlayer distance of 0.40 nm. The surface porosity from Brunauer–Emmett–Teller (BET) analysis ( $N_2$ , 77 K) was 171, 166, and  $266 \text{ m}^2/\text{g}$  for  $\text{Cu}_3\text{HHTP}_2$ ,  $\text{Ni}_3\text{HHTP}_2$ , and  $\text{Co}_3\text{HHTP}_2$ , respectively (Figure S6).<sup>29</sup>

Thermal gravimetric analysis (TGA) revealed increased thermal stability of PCPs compared to the HHTP precursor (Figure S13). Electron paramagnetic resonance (EPR) spectroscopy showed ligand-centered radicals in  $\text{Ni}_3\text{HHTP}_2$  and  $\text{Co}_3\text{HHTP}_2$ , and a metal centered radical in  $\text{Cu}_3\text{HHTP}_2$ ; limited paramagnetism was observed for the HHTP ligand (Figure S11). Attenuated total reflectance infrared spectroscopy (ATR-IR) confirmed the disappearance of the S–H stretching vibration at  $2510 \text{ cm}^{-1}$  upon metal coordination (Figure S12).<sup>21,22</sup> Bulk conductivity of  $2.4 \times 10^{-9}$ ,  $3.6 \times 10^{-4}$ , and  $2.4 \times 10^{-8} \text{ S/cm}$  for  $\text{Co}_3\text{HHTP}_2$ ,  $\text{Ni}_3\text{HHTP}_2$ , and  $\text{Cu}_3\text{HHTP}_2$ , respectively, suggested reasonable ability for charge transport.

Cyclic voltammetry (CV) studies in a nonaqueous environment ( $-2.0$  to  $+2.0 \text{ V}$  in MeCN) established the electroactive nature of the materials in this study (Figure 2A, and Figure S15). We identified the presence of three distinct spectral features: (i) two redox peaks at oxidative potentials above  $+0.70 \text{ V}$ ; (ii) one redox transition at potentials below  $+0.20 \text{ V}$  on the anodic scan and (iii) lack of well-defined redox peaks during the cathodic scans.

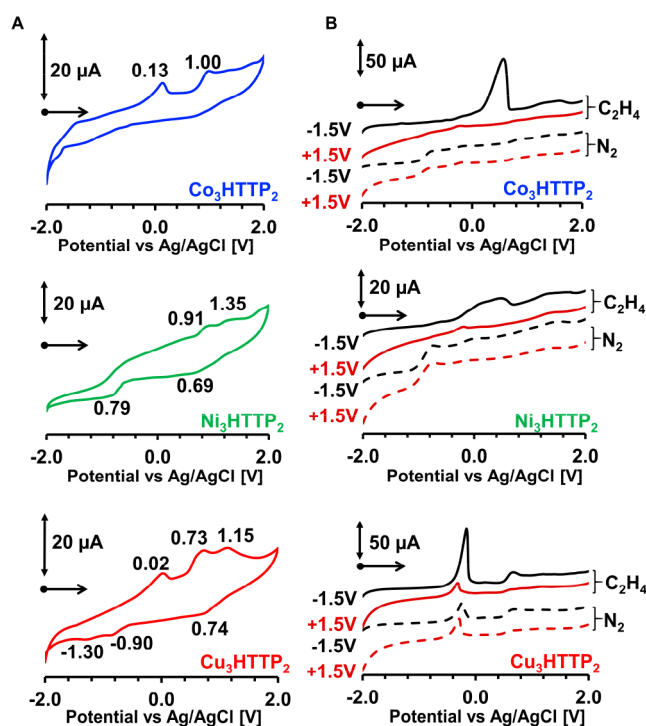


**Figure 2.** Electrochemical characterization of  $\text{M}_3\text{HHTP}_2$  PCPs. Arrows indicate directions of scans. The double headed arrows indicate the magnitude of current. (A) Cyclic voltammograms for  $\text{Co}_3\text{HHTP}_2$  in blue,  $\text{Ni}_3\text{HHTP}_2$  in green, and  $\text{Cu}_3\text{HHTP}_2$  in red; scan rate:  $10 \text{ mV/s}$ . (B) Linear sweep voltammograms (scan rate  $50 \text{ mV/s}$ ) in the presence of dissolved  $\text{N}_2$  (dashed lines) and  $\text{C}_2\text{H}_4$  (solid lines). PCPs are either preoxidized (red) or prereduced (black). All measurements were performed in  $0.1 \text{ mM TBAPF}_6$  in MeCN under  $\text{N}_2$  (5 scans).  $3 \text{ mm}$  diameter glassy carbon electrode, platinum wire, and Ag/AgCl electrodes were used as the working, counter, and reference electrode, respectively.

Redox transitions found at higher oxidative potentials ( $> +0.70 \text{ V}$ ) closely matched the redox peaks observed for the organic precursors used to produce  $\text{M}_3\text{HHTP}_2$  or  $\text{M}_3\text{HHTP}_2$  PCPs (Figure 2A, Figures S14–15). The distinct negative shift compared to the free ligand in the oxidation potential of the PCPs may indicate that the electron transfer is largely stabilized in the PCPs.<sup>36</sup> The presence of redox transitions found at lower oxidative potentials ( $< +0.20 \text{ V}$ ) in Figure 2A could originate from (i) redox activity of the metal centers within the PCPs,<sup>37</sup> (ii) coexistence of multiple redox processes due to defects (e.g., exposed leading edges, such as open metal and ligand sites in the framework),<sup>38</sup> and (iii) redox active impurities permanently embedded within the framework. The lack of well-defined peaks on the cathodic scan may indicate irreversibility of the electrochemical system, or that the electron transfer process is followed directly by a chemical reaction in which nonredox active species are formed.<sup>39</sup>  $\text{M}_3\text{HHTP}_2$  PCPs were stable to at least five consecutive CV cycles (Figure S24).

Next, we proceeded to examine the interactions of PCPs with  $\text{C}_2\text{H}_4$  in solution (Figure 2B, Figures S17–S18). Due to limited solubility of ethylene in organic and aqueous solvents ( $\sim 1 \text{ mM}$ ),<sup>40</sup> we employed a preconcentration step to enhance the electrochemical response (Figures S19–S20, S22).<sup>41,42</sup> Figure 2B compares the linear sweep voltammetry (LSV) responses for the  $\text{M}_3\text{HHTP}_2$  materials immobilized on glassy carbon electrodes after  $6 \text{ min}$  accumulation time at  $-1.5$  and  $+1.5 \text{ V}$  under  $\text{N}_2$  and  $\text{C}_2\text{H}_4$  in MeCN. In the presence of  $\text{C}_2\text{H}_4$ , preconcentration at  $-1.5 \text{ V}$  led to a notable increase in peak current intensity (Figure 2B, solid black line). Reversing the potential from  $-1.5$  to  $+1.5 \text{ V}$  during preconcentration, diminished the peak current intensity (solid red line) to a level of being indistinguishable from the results in the presence of  $\text{N}_2$  (dashed lines).

Though the voltammetric response in Figure 2B suggested the presence of  $\text{C}_2\text{H}_4/\text{M}_3\text{HHTP}_2$  interactions, we employed  $\text{M}_3\text{HHTP}_2$  MOFs to gain additional insight into the mechanistic details of this electrochemically driven transformation. This control can (i) probe the possibility of ethylene capture through the formation of the  $\pi$ -complex with the metal center in the PCPs, and (ii) examine the role of chalcogen atoms (S vs O) in the capture process. To test these possibilities, we held the electrode with drop-cast layer of  $\text{M}_3\text{HHTP}_2$  for  $120 \text{ s}$  at either  $-1.5$  or  $+1.5 \text{ V}$  in  $\text{N}_2$  or  $\text{C}_2\text{H}_4$  (Figure S23). In each case,  $\text{M}_3\text{HHTP}_2$  controls did not produce a change in response. We, therefore, conclude that the similarities in LSV response for all HHTP-based materials reinforce that S atoms of the metal bis(dithiolene) complex are critical to the observed electrochemical performance in the presence of  $\text{C}_2\text{H}_4$ .

The results from solution-based electrochemical measurements are subject to complications due to several experimental factors, including (i) effect of solvent, (ii) choice of electrolyte, (iii) solubility of gas, and (iv) requirement for three electrode configuration, making electrochemical capture of ethylene in solution a complex process. We proceeded to develop a strategy that overcomes these complexities by integrating each  $\text{M}_3\text{HHTP}_2$  PCP into two types of solid-state devices (Figure S25): (i) PCP-coated conductive slides ( $2.5 \text{ cm} \times 1.5 \text{ cm}$  with  $5 \text{ mg}$  loading of  $\text{M}_3\text{HHTP}_2$ ), and (ii) the compressed pellet ( $6 \text{ mm}$  diameter,  $62 \text{ mg}$ ,  $1.45 \text{ mm}$  thickness). We reasoned that stimulating these forms of material with applied potential would enable electrically actuated reactivity of the PCP with  $\text{C}_2\text{H}_4$ .

Capture and release of ethylene was achieved by delivering electrical potential (+2.0 or −2.0 V) to the solid-state device. We then used Henry's law for gas–liquid partitioning to quantify the amount of released  $C_2H_4$  by NMR.<sup>43</sup> Only electrochemically oxidized  $M_3HHTTP_2$  PCPs were capable of capturing  $C_2H_4$  (Figure 3D,E). Despite the 10-fold difference in

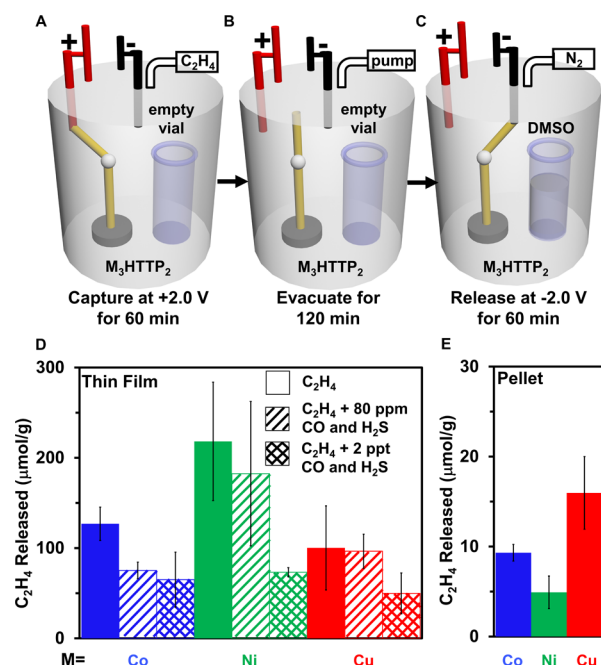


**Figure 3.** Experimental design and demonstration for solid-state electrochemical capture and release of ethylene. (A) The setup comprises the PCPs positioned under ethylene atmosphere ( $\sim 1$  atm) in a sealed container. Applied electrical potential (+2.0 V) to the material facilitates ethylene capture. (B) Switching off the power, and evacuating at  $1.5 \times 10^{-3}$  Torr removes all unbound ethylene. (C) Refilling of the container with  $N_2$ , and addition of deuterated dimethyl sulfoxide ( $DMSO-d_6$ ) enables monitoring of electrochemical release by NMR. Subsequent reduction at −2.0 V promotes ethylene release. (D,E) The amount of ethylene quantified in the electrochemical capture/release experiment in the absence and presence of interferents (80 ppm and 2 ppt of CO and  $H_2S$ ) by thin films (D) and pellets (E).

the amounts of electrochemically captured  $C_2H_4$  in  $\mu\text{mol/g}$  captured by thin films (Figure 3D) as compared to pellets (Figure 3E), the similarity in uptake in moles (300–1100 nmol) by these two devices (Tables S4–S5) suggested that the exposed surface area (rather than the bulk) dominated the capture process. Analysis of pellets by BET (Figure S7) showed  $\sim 30$  times reduction in porosity upon compression, and confirmed the role of surface-dominated process.

The application of electrical potential was essential for driving the capture process in the solid-state. No  $C_2H_4$  capture was detected in the absence of applied potential, or the case of omission of either the oxidation or reduction steps (Section IV in SI, Figures S33–S38). Two control materials— $M_3HHTTP_2$  MOFs or HHTTP ligand—did not produce observable capture (SI Section IV, Figures S31–S32, S39). These findings confirm the essential role of metal bis(dithiolene) complex in the electrochemically driven capture.

The presence of gaseous inhibitors above 10 ppm can poison metal-based catalysts in  $C_2H_4$  purification.<sup>2,3</sup> We thus evaluated the solid-state performance of  $M_3HHTTP_2$  PCPs for  $C_2H_4$  capture in the presence of interfering poisoning agents ( $H_2S$

and CO). We exposed each of the PCPs to a mixture of gases comprising  $H_2S$ , CO (80 ppm or 2 ppt), and ethylene for 60 min at +2.0 V (applied potential), and then measured the amount of ethylene recovered in the NMR solvent immediately after the release step (−2.0 V for 60 min). Remarkably, the presence of 80 ppm of gaseous poisons reduced the performance of thin films only by 40%, 15%, and 3% for  $Co_3HHTTP_2$ ,  $Ni_3HHTTP_2$ , and  $Cu_3HHTTP_2$  PCPs (Figure 3D). Even in the presence of 2 ppt of  $H_2S$  and CO, the materials still maintained 35–50% of their function (Figure 3D, Tables S4–S5). Together, these findings indicate that the  $M_3HHTTP_2$  materials retain their function in a complex environment, and resist poisoning by interferents.<sup>44</sup>

In conclusion, this paper describes the first experimental implementation of PCPs to achieve electrochemically driven capture and release of ethylene in solution and at the solid–gas interface. This method has five distinct advantages for electrochemically controlled molecular capture: (i) it is compatible both with the solution-phase capture in the presence of electrolytes and with the direct solid-state capture in the absence of electrolytes, (ii) it is resistant to poisoning by reactive gases, such as CO and  $H_2S$ , (iii) it enables preconcentration of the olefin within a PCP, (iv) it employs relatively low overpotentials in the range of −2.0 to +2.0 V, and (v) it utilizes a class of modular porous materials that can be further optimized for performance through strategic design.

The observed unoptimized  $C_2H_4$  uptake efficiency of  $M_3HHTTP_2$  PCPs drop-casted films (ranging from 0.10 to 0.22 mmol/g, Table S4) is approximately 1 order of magnitude below FeMOF-74 (6.8 mmol/g at 1 bar)<sup>45</sup> and SIFSIX-1-Cu (8.5 mmol/g at 1 bar),<sup>46</sup> and comparable to other microporous scaffolds.<sup>47,48</sup> The distinguishing feature of the process presented herein is its compatibility with low pressure and ambient temperature.<sup>49</sup> We expect that further investigation of the proof-of-concept methodology presented herein may enhance innovation in materials design, chemical sensing, preconcentration, purification, and catalysis.

## ■ ASSOCIATED CONTENT

### Supporting Information

The Supporting Information is available free of charge on the ACS Publications website at DOI: 10.1021/jacs.7b08102.

Experimental details, nitrogen isotherms, spectroscopic, microscopic, elemental, and electrochemical characterization (PDF)

## ■ AUTHOR INFORMATION

### Corresponding Author

\*katherine.a.mirica@dartmouth.edu

### ORCID

Katherine A. Mirica: 0000-0002-1779-7568

### Notes

The authors declare no competing financial interest.

## ■ ACKNOWLEDGMENTS

K.A.M. acknowledges the funds provided by Dartmouth College, and the Walter and Constance Burke Research Initiation Award. The authors thank Alice J. Hsu for the help with HHTTP synthesis and the initial efforts in preparing  $M_3HHTTP_2$  PCPs.



## ■ REFERENCES

- (1) Bodke, A. S. *Science* **1999**, 285, 712.
- (2) *Handbook of petroleum refining processes*, 3rd ed.; Meyers, R. A., Ed.; McGraw-Hill: New York, 2004.
- (3) Speight, J. In *Kirk-Othmer Encyclopedia of Chemical Technology*; Seidel, A., Ed.; John Wiley & Sons, Inc.: Hoboken, NJ, 2000.
- (4) Suzuki, T.; Noble, R. D.; Koval, C. A. *Inorg. Chem.* **1997**, 36, 136.
- (5) Wang, K.; Stiefel, E. I. *Science* **2001**, 291, 106.
- (6) Sholl, D. S.; Lively, R. P. *Nature* **2016**, 532, 435.
- (7) Herm, Z. R.; Bloch, E. D.; Long, J. R. *Chem. Mater.* **2014**, 26, 323.
- (8) Schrauzer, G. N.; Mayweg, V. P. *J. Am. Chem. Soc.* **1965**, 87, 1483.
- (9) Stiefel, E. I. *Diithiolene Chemistry: Synthesis, Properties, and Applications*. In *Progress in Inorganic Chemistry*; John Wiley & Sons, Inc.: Hoboken, NJ, 2004; Vol. 52.
- (10) Eisenberg, R.; Gray, H. B. *Inorg. Chem.* **2011**, 50, 9741.
- (11) Dang, L.; Shibl, M. F.; Yang, X.; Alak, A.; Harrison, D. J.; Fekl, U.; Brothers, E. N.; Hall, M. B. *J. Am. Chem. Soc.* **2012**, 134, 4481.
- (12) Raju, R. K.; Sredojevic, D. N.; Moncho, S.; Brothers, E. N. *Inorg. Chem.* **2016**, 55, 10182.
- (13) Dang, L.; Shibl, M. F.; Yang, X.; Harrison, D. J.; Alak, A.; Lough, A. J.; Fekl, U.; Brothers, E. N.; Hall, M. B. *Inorg. Chem.* **2013**, 52, 3711.
- (14) Harrison, D. J.; Lough, A. J.; Nguyen, N.; Fekl, U. *Angew. Chem., Int. Ed.* **2007**, 46, 7644.
- (15) Boyer, J. L.; Cundari, T. R.; DeYonker, N. J.; Rauchfuss, T. B.; Wilson, S. R. *Inorg. Chem.* **2009**, 48, 638.
- (16) Kunkely, H.; Vogler, A. *Inorg. Chim. Acta* **2001**, 319, 183.
- (17) Dang, L.; Yang, X.; Zhou, J.; Brothers, E. N.; Hall, M. B. *J. Phys. Chem. A* **2012**, 116, 476.
- (18) Grapperhaus, C. A.; Ouch, K.; Mashuta, M. S. *J. Am. Chem. Soc.* **2009**, 131, 64.
- (19) Tang, Q.; Zhou, Z. *J. Phys. Chem. C* **2013**, 117, 14125.
- (20) Moncho, S.; Brothers, E. N.; Hall, M. B. *J. Mol. Model.* **2015**, 21, 107.
- (21) Dong, R.; Pfeiffermann, M.; Liang, H.; Zheng, Z.; Zhu, X.; Zhang, J.; Feng, X. *Angew. Chem., Int. Ed.* **2015**, 54, 12058.
- (22) Clough, A. J.; Yoo, J. W.; Mecklenburg, M. H.; Marinescu, S. C. *J. Am. Chem. Soc.* **2015**, 137, 118.
- (23) Downes, C. A.; Marinescu, S. C. *J. Am. Chem. Soc.* **2015**, 137, 13740.
- (24) Downes, C. A.; Marinescu, S. C. *Dalton Trans* **2016**, 45, 19311.
- (25) Kobayashi, Y.; Jacobs, B.; Allendorf, M. D.; Long, J. R. *Chem. Mater.* **2010**, 22, 4120.
- (26) Kambe, T.; Sakamoto, R.; Kusamoto, T.; Pal, T.; Fukui, N.; Hoshiko, K.; Shimojima, T.; Wang, Z.; Hirahara, T.; Ishizaka, K.; Hasegawa, S.; Liu, F.; Nishihara, H. *J. Am. Chem. Soc.* **2014**, 136, 14357.
- (27) Cui, J.; Xu, Z. *Chem. Commun.* **2014**, 50, 3986.
- (28) Huang, X.; Sheng, P.; Tu, Z.; Zhang, F.; Wang, J.; Geng, H.; Zou, Y.; Di, C.; Yi, Y.; Sun, Y.; Xu, W.; Zhu, D. *Nat. Commun.* **2015**, 6, 7408.
- (29) Clough, A. J.; Skelton, J. M.; Downes, C. A.; de la Rosa, A. A.; Yoo, J. W.; Walsh, A.; Melot, B. C.; Marinescu, S. C. *J. Am. Chem. Soc.* **2017**, 139, 10863.
- (30) Pal, T.; Kambe, T.; Kusamoto, T.; Foo, M. L.; Matsuoka, R.; Sakamoto, R.; Nishihara, H. *ChemPlusChem* **2015**, 80, 1255.
- (31) Zhao, M.; Wang, A.; Zhang, X. *Nanoscale* **2013**, 5, 10404.
- (32) Smith, M. K.; Jensen, K. E.; Pivak, P. A.; Mirica, K. A. *Chem. Mater.* **2016**, 28, 5264.
- (33) Hmadeh, M.; Lu, Z.; Liu, Z.; Gándara, F.; Furukawa, H.; Wan, S.; Augustyn, V.; Chang, R.; Liao, L.; Zhou, F.; Perre, E.; Ozolins, V.; Suenaga, K.; Duan, X.; Dunn, B.; Yamamoto, Y.; Terasaki, O.; Yaghi, O. M. *Chem. Mater.* **2012**, 24, 3511.
- (34) Sun, L.; Campbell, M. G.; Dincă, M. *Angew. Chem., Int. Ed.* **2016**, 55, 3566.
- (35) Campbell, M. G.; Sheberla, D.; Liu, S. F.; Swager, T. M.; Dincă, M. *Angew. Chem., Int. Ed.* **2015**, 54, 4349.
- (36) Sato, M.; Nagata, T.; Tanemura, A.; Fujihara, T.; Kumakura, S.; Unoura, K. *Chem. - Eur. J.* **2004**, 10, 2166.
- (37) Loera-Serna, S.; Oliver-Tolentino, M. A.; de Lourdes López-Núñez, M.; Santana-Cruz, A.; Guzmán-Vargas, A.; Cabrera-Sierra, R.; Beltrán, H. I.; Flores, J. *J. Alloys Compd.* **2012**, 540, 113.
- (38) Peng, Z.; Yi, X.; Liu, Z.; Shang, J.; Wang, D. *ACS Appl. Mater. Interfaces* **2016**, 8, 14578.
- (39) Bard, A. J.; Faulkner, L. R. *Electrochemical methods: fundamentals and applications*, 2nd ed.; Wiley: New York, 2001.
- (40) Davis, J. E.; McKetta, J. J. *J. Chem. Eng. Data* **1960**, 5, 374.
- (41) Fogg, A. G. *Anal. Proc.* **1994**, 31, 313.
- (42) Wang, J.; Mahmoud, J. S. *J. Electroanal. Chem. Interfacial Electrochem.* **1986**, 208, 383.
- (43) Renon, H.; Lenoir, J. Y.; Renault, P. *J. Chem. Eng. Data* **1971**, 16, 340.
- (44) *Separation and purification technology*; Li, N. N.; Calo, J. M., Eds.; M. Dekker: New York, 1992.
- (45) Bloch, E. D.; Queen, W. L.; Krishna, R.; Zadrozny, J. M.; Brown, C. M.; Long, J. R. *Science* **2012**, 335, 1606.
- (46) Cui, X.; Chen, K.; Xing, H.; Yang, Q.; Krishna, R.; Bao, Z.; Wu, H.; Zhou, W.; Dong, X.; Han, Y.; Li, B.; Ren, Q.; Zaworotko, M. J.; Chen, B. *Science* **2016**, 353, 141.
- (47) Li, B.; Zhang, Y.; Krishna, R.; Yao, K.; Han, Y.; Wu, Z.; Ma, D.; Shi, Z.; Pham, T.; Space, B.; Liu, J.; Thallapally, P. K.; Liu, J.; Chrzanowski, M.; Ma, S. *J. Am. Chem. Soc.* **2014**, 136, 8654.
- (48) Bao, Z.; Chang, G.; Xing, H.; Krishna, R.; Ren, Q.; Chen, B. *Energy Environ. Sci.* **2016**, 9, 3612.
- (49) Liao, Y.; Zhang, L.; Weston, M. H.; Morris, W.; Hupp, J. T.; Farha, O. K. *Chem. Commun.* **2017**, 53, 9376.